ORIGINAL PAPER

Electrochemical Scanning Tunneling Microscopy as a Tool for the Detection of Active Electrocatalytic Sites

Thorsten O. Schmidt[1] · Richard W. Haid[1] · Elena L. Gubanova[1] · Regina M. Kluge[1] · Aliaksandr S. Bandarenka[1,2]

Abstract

To advance meaningful guidelines in the design of electrocatalytically active catalysts, a knowledge of the nature of active sites is the starting point. However, multiple factors such as material composition, site coordination, electrolyte effects, the support material, surface strain, and others influence catalytic behavior. Therefore, the identification of active sites can be complex. A substantial contributor can be in-situ experiments, which are able to identify active centers in a specific system while the reaction takes place. An example of such a technique is electrochemical scanning tunneling microscopy (EC-STM), which relates locally confined noise features to local electrocatalytic activity. In this work, we spotlight recent achievements of this technique with respect to palladium (Pd) surfaces for the hydrogen reduction reaction, where strain due to hydride formation comes into play in addition to surface coordination. Secondly, we demonstrate the high resolution of the technique on graphite-based surfaces. Here, edge sites are particularly active. Thus, with the EC-STM technique, we take strain effects (like on Pd) or effects of coordination (like on carbon) into account. Therefore, we can determine active sites with great accuracy under reaction conditions.

Keywords Active site · Hydrogen evolution reaction · Electrochemical scanning tunneling microscopy · In-situ method · Palladium · Carbon

1 Introduction

Renewable energy is inevitable for a more sustainable and worldwide accessible energy provision. However, due to intermittency, energy storage is necessary. Due to its large energy density, hydrogen is considered a promising candidate [1]. Electrocatalytic water splitting is a major element for large-scale production of 'green' hydrogen from renewable electricity [2]. Among the involved electrochemical half-cell reactions is the cathodic hydrogen evolution reaction (HER). The HER requires an active, stable, and low-cost electrocatalyst to increase the electrolyzer efficiency. State-of-the-art materials are platinum (Pt) and palladium (Pd) [3], but also cheap materials such as carbon [4, 5] are considered. Hydrogen adsorption and subsequently also the HER can depend on the structure of the catalyst surface [6, 7]. Therefore, to design an effective catalyst, it is essential to know which sites on the catalytic surface are active.

For active site identification, ex-situ methods such as scanning electron microscopy, Raman spectroscopy, Fourier-transform infrared spectroscopy, x-ray photoelectron spectroscopy, and x-ray diffraction are employed [8]. Beyond, in-situ techniques like scanning electrochemical cell microscopy, where a miniature electrochemical cell assesses the local reactivity [9], and electrochemical scanning tunneling microscopy (EC-STM), in which structural changes or self-activation can be observed under reaction conditions [10] are versatile techniques. The major difficulty is that the nature of active sites can depend on coordination, ligand and strain effects, particle size, electrolyte interactions, and many more [11].

Therefore, assessing the local activity of different surface sites under reaction conditions, paired with high resolution, is a strong approach. We first introduce an EC-STM technique that can do so via the analysis of noise features.

✉ Regina M. Kluge
   regina.kluge@ph.tum.de

✉ Aliaksandr S. Bandarenka
   bandarenka@ph.tum.de

[1] Physik-Department ECS, Technische Universität München, James-Franck-Straße 1, 85748 Garching, Germany

[2] Catalysis Research Center TUM, Ernst-Otto-Fischer-Straße 1, 85748 Garching, Germany

Afterward, we showcase the ability of the technique for the HER. As model systems, we chose Pd, known as a complex system and for its ability to form hydrides. Besides, we demonstrate on highly oriented pyrolytic graphite (HOPG) that active sites can be distinguished with atomic resolution.

2 Method: Electrochemical Scanning Tunneling Microscopy for Active Site Identification

In scanning tunneling microscopy (STM), an atomically sharp scanning probe moves across a conductive sample to provide the electronic topology. Depending on the mode, the tip-sample distance is adjusted to the tunneling current, or the tunneling current is recorded at a fixed tip-sample distance. The tunneling current is highly sensitive to the width of the tunneling gap (exponential dependence). Therefore, it was the first technique capable of achieving atomic resolution of a surface in real space [12, 13].

EC-STM profits from this high resolution and combines the 'conventional' STM with an electrochemical cell, including a reference (RE) and a counter electrode (CE). Instead of a vacuum or air, an electrolyte serves as the tunnel medium. A bi-potentiostat controls the potentials between tip and sample, influencing the tunneling current, and between the sample and RE, allowing control over electrochemical reactions at the sample/electrolyte interface. The tip itself is insolated with an inert material, preventing any Faradaic reactions on the tip, which could falsify the tunnel current emanating from the sample.

In addition to the sample and tip work function, tip-sample distance, tunneling voltage, etc., the tunneling current depends on the tunneling medium, such as the electrolyte structure, movement of chemical species across the tunneling gap and adsorbed species on the surface [14–20]. Considering those dependencies, it becomes understandable why EC-STM provides valid information when performed under electrocatalytic reaction conditions. An ongoing reaction persistently changes the composition and structure of the tunneling medium. Consequently, fluctuations of the tunneling current caused by the resulting changes in the electrochemical properties within the tunneling barrier lead to a temporary retraction of the STM tip. Due to the temporal random occurrence of electrochemical events, a noise-like behavior of the STM signal is observed. These changes are the most pronounced at the position where the electrocatalytic reactions occur: at the active centers. Therefore, information about the local activity can be extracted by evaluating the noise features appearing during such a reaction.

Figure 1a sketches the working principle of the noise-EC-STM (n-EC-STM) technique. As described above, the electrolyte between the tip and sample serves as the tunneling medium while the tip is scanning across the surface. Dependent on the chosen sample potential with respect to the RE, the reaction of interest is either enabled ('On') or not ('Off'). If the reaction is hindered, the signal is recorded without distortion, and, e.g., the morphology of a step edge can be mapped (black curve sketched in the tunneling gap). If the reaction is ongoing, distinct noise features appear at the position of the active sites. In the example, the blue atoms at the top of the step edge are active. Therefore, the signal under reaction conditions (blue curve sketched in the tunneling gap) is a superposition of the step edge morphology and the distinct noise features at the active step-top sites. The reason for the distinct noise features is the dependence of the changes in the electrolyte on the tunneling barrier, as discussed above. The n-EC-STM technique can be used to monitor active areas and quantify local activity values. An example is given in Fig. 1b, c on the model system Pt(111) for the oxygen reduction reaction (ORR) in 0.1 M perchloric acid ($HClO_4$) [23]. For this system, the sites with higher coordination in the vicinity of step edges were identified as active [21, 22], which is in accordance with the higher noise level at the step sites in Fig. 1b.

To quantify the noise level for each data set (reaction 'On'/'Off', step or terrace sites), the STM signal was derived with respect to adjacent data points, according to

$$\left(\frac{\partial z}{\partial x}\right)_{t_1} = \frac{1}{2}\left[\frac{z_2 - z_1}{x_2 - x_1} + \frac{z_1 - z_0}{x_1 - x_0}\right]$$

where (x_0, z_0), (x_1, z_1) and (x_2, z_2) are three successive data points with scan direction x and tip-sample distance z. In the next step, histograms were compiled from the signal derivatives, as shown in Fig. 1c. To compare data sets of unequal sizes, each histogram was divided by the number of data points to 'normalized counts'. The histograms were fitted by Gaussian curves, and the full width at half maximum (FWHM) and the height of the Gaussian fit served as descriptors of the noise level. If spikes are present in the scan, a large number of different slopes arise. Consequently, for an elevated noise level in the STM signal, the derivatives are scattered widely around zero. The corresponding histogram is broader and of lower intensity. Analog, this quantification is possible in constant current mode using the derivative of the height signal with respect to adjacent data points. With this approach, it is possible to assign a number to the noise level of a certain signal. Applied to the Pt(111) example for the ORR, step sites are indeed more active as they show a broader histogram than the terrace sites
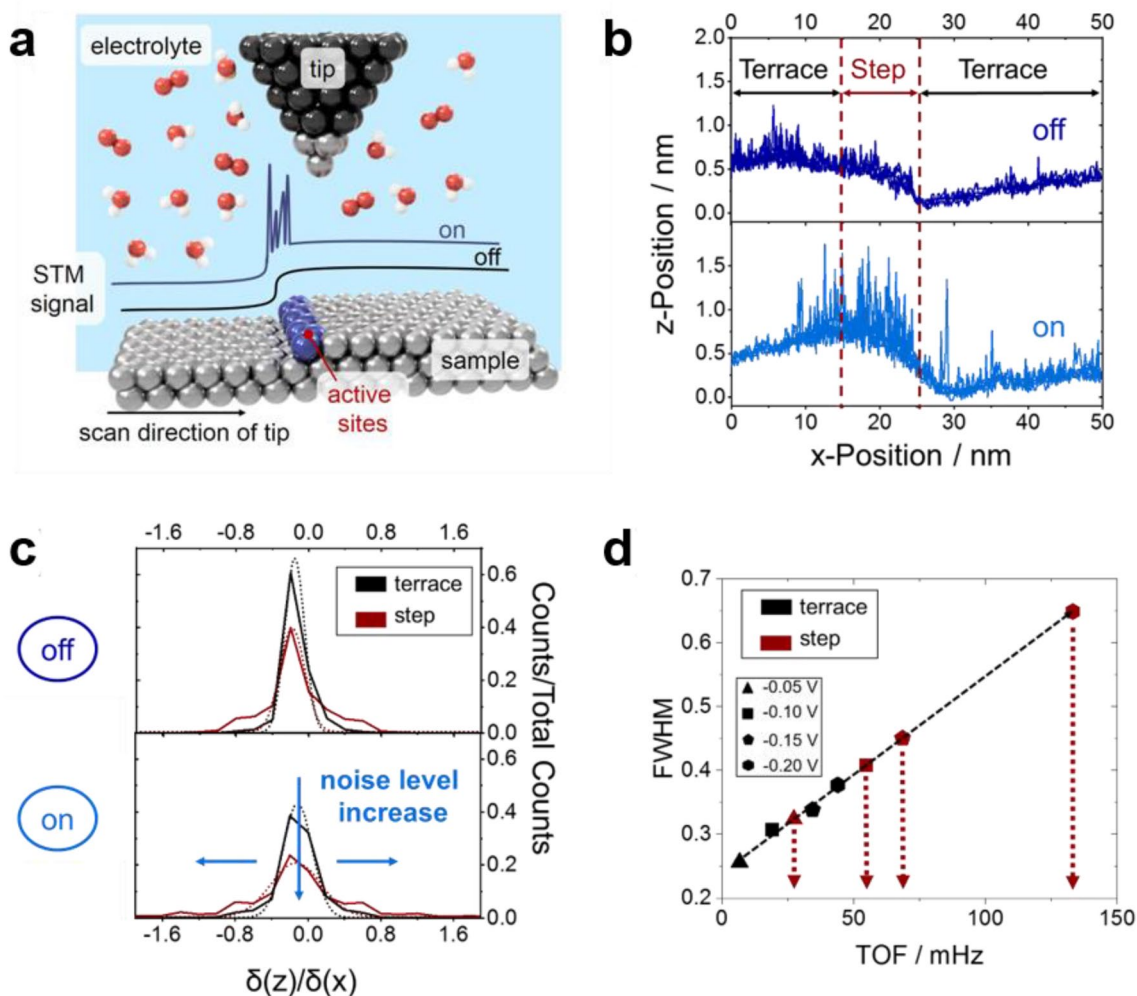
Fig. 1 n-EC-STM principle for the detection and quantification of local activity. **a** The EC-STM signal is obtained by a tip scanning across a conductive sample with the tunneling gap in-between filled by the electrolyte. The tip is insulated against chemical reactions e.g. by a layer of wax. If the potential between the sample and RE is chosen such that no reaction takes place ('Off'), the signal is unperturbed (black line in tunneling gap). However, if a reaction is allowed ('On'), distinct noise features appear at the position of the active sites. In this example, the active sites are colored in blue at the top of the step edge. **b** Example of an n-EC-STM measurement under ORR conditions on a Pt(111) surface in 0.1 M HClO$_4$. An increased noise level is observed near the step for reaction 'On'. Therefore, step sites are

more active than terrace sites for this system. **c** Histograms for the data in (**b**) confirm that step sites are more active than terrace sites because the histogram for step sites under reaction conditions (red curve in the lower graph) is broader and less intense than for terrace sites (black curve). Details can be found in the main text. **d** Further experiments for the same system as **b**, **c** confirm that the FWHM of the histogram, quantifying the noise level, is linearly related to the local TOF. This instant serves as means for a local quantification of activity using EC-STM. Data in (**b–d**) and the applied potentials published in reference [23]. . © 2020 The Authors Published by Wiley-VCH GmbH

in Fig. 1c. This kind of experiment was repeated for various step sites and various applied sample potentials. The FWHM served as a descriptor for the noise level. As a descriptor for the activity, the turnover frequency (TOF), defined as the number of reaction events per active site and per time unit for a fixed set of reaction conditions [24], was chosen. For the terrace sites, the TOF was calculated from the overall sample current, assuming a low overall number of nonterrace sites (step and defect sites) on the annealed Pt(111) surface. Importantly, a linear trend could be established

between FWHM and TOF from a set of applied potentials within one measurement series. By assessing the noise level of the step edges and using the noise-activity relation from adjacent terrace sites, one can extrapolate the local activity of the step sites. The relation between FWHM and TOF is shown in Fig. 1d for the same data set as in Fig. 1b, c. The noise-activity relation did not only serve to very locally extract the activity of a certain category of surface sites but also confirms that the noise features in the EC-STM signal are indeed caused by an electrocatalytic activity. These

findings were confirmed by Agnoli et al. [25, 26], who state that the electrocatalytic influence on the tunneling current takes the form of a first-order perturbation at low overpotentials. With their quantification approach, they can assess the onset potential, the Tafel slope, and the TOF locally for different surface geometries.

In summary, the EC-STM technique serves as a viable tool to identify active sites with high resolution while at the same time being able to assess the surface morphology.

3 Experimental Details

The samples investigated in this work were Pd(111) and Pd(100) single crystals (both Ø 5 mm, 99.999%, MaTecK, Germany), and HOPG (mosaic spread value 3.5°, mosaic spread accuracy ± 1.5°, sample size $10 \times 10 \times 1$ mm^3, Nano-AndMore GmbH, Germany).

A Nanoscope III SPM Multimode (Veeco Instruments) connected to a Nanoscope IIID controller and a Veeco Nanoscope Universal bipotentiostat was used for the n-EC-STM experiments. The sample was clamped between a stainless steel plate and a polytetrafluoroethylene (PTFE) ring. This resulted in a miniature electrochemical cell, which can host the electrolyte. For all measurements, 0.1 M HClO$_4$ (70% HClO$_4$, Suprapur, Merck, Germany) was used as the electrolyte and prepared by the dilution with ultrapure water (18.2 MΩ cm, Evoqua Milli-Q). Two wires were immersed into the electrolyte and acted as RE and CE. The RE was Pt (Ø 0.5 mm, 99.99%, MaTecK, Germany). The CE was a carbon rod (Ø 0.5 mm, 99.95%, Goodfellow GmbH) or a curled palladium wire (Ø 0.25 mm, 99.95%, MaTecK, Germany) for the measurements on HOPG or the palladium single crystals, respectively. The STM tips were mechanically ripped from a platinum-iridium wire (Pt80/Ir20, Ø = 0.25, 99.9 + %, Goodfellow GmbH) with a side cutter. The tip was insolated with Apiezon® wax [27].

Since STM is not an element-sensitive technique, well-defined model surfaces are needed for profound findings. Therefore, specific preparations are required to clean and smoothen the sample. For the palladium single crystals, a controlled annealing temperature of approximately 950° C under the exclusion of oxygen was required. For this purpose, two different heating systems were applied: a high-frequency induction heater (20–80 kHz, 15 KW–EQ-SP-15A, MTI, USA) and a tube furnace (Heraeus Instruments RO 7/50). In both, the Pd surfaces were annealed in an argon atmosphere (Argon 5.0, Westfalen, Germany). The annealed surface was protected by a drop of electrolyte before the electrochemical measurements. The HOPG surface was prepared by removing the first layers with adhesive tape. More details are available in references [28, 29].

4 Results & Discussion: n-EC-STM Measurements for the HER

In the following, we demonstrate the in-situ technique for the HER. First, we focus on Pd(111) and Pd(100) model surfaces and showcase the different noise behavior on sites of different coordination. Second, we demonstrate the atomic resolution of the technique on a graphite material.

4.1 Palladium Catalyst Surfaces: In-Situ Imaging and Identification of Active Sites

For structure-sensitive reactions, the local activity strongly depends on the coordination of the surface sites. The reason is that surface site coordination is for many reaction intermediates directly related to the binding strength between the surface site and the reaction intermediate [30]. The Sabatier principle concludes that binding strength should be optimal at active sites and thus also coordination. Therefore, n-EC-STM measurements can contribute to finding the optimal surface geometry by relating step and terrace sites in the same image. In the case of Pd hydride formation, strain plays a role, which can also influence the nature of active sites [28]. In the here-presented study, cyclic voltammetry measurements in Ar-saturated 0.1 M HClO$_4$ provided enough hydrogen absorption and the subsequent release of strain to convert an atomically flat surface of a freshly annealed Pd crystal into a 'hilly' surface. Figure 2 illustrates this change in morphology by STM measurements for reaction 'Off' on Pd(111) (Fig. 2a, b) and Pd(100) (Fig. 2c, d) before (Pd) and after 8 or 5 cycles (Pd$_c$), respectively.

This restructured morphology also leads to a change in the location of the active sites (cf. ref. [28]). However, to keep it simple, under reaction conditions, we only consider surface coordination without strain by measuring a freshly annealed sample and performing n-EC-STM measurements at the onset of the HER to avoid the influence of hydride formation.

The nature of active sites on Pd surfaces was investigated on the two model surfaces with orientations (111) and (100). For the n-EC-STM experiments, the surfaces were freshly annealed and protected from oxygen as described in the section '3'. The used electrolyte was 0.1 M HClO$_4$. The STM measurement in Fig. 3a, b includes two steps on Pd(111) with a height of 2.2 nm, which corresponds to approximately eight Pd layers
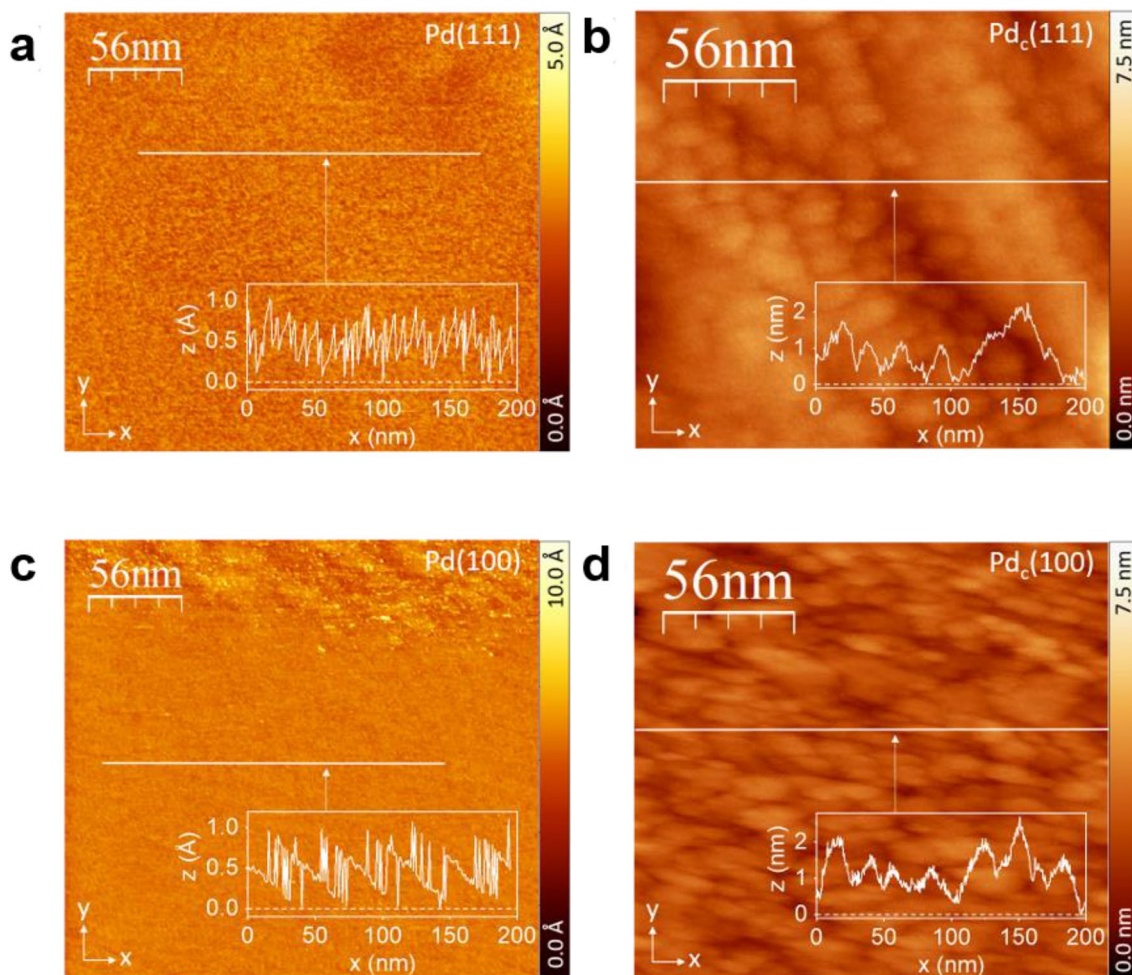
Fig. 2 STM measurements for reaction 'Off' of annealed Pd before (**a**, **c**) and after (**b**, **d**) cyclic voltammetry (8 or 5 cycles, respectively) performed at a potential between 0.2 and 1.2 V versus a reversible hydrogen electrode (RHE) and a scan rate of 50 mV s^{-1}. The inset line scans show the height profile of each surface at the position indicated with the solid white line. While the freshly annealed surfaces (**a**, **c**) are mostly atomically flat, the surfaces after cycling (Pd$_c$) in **b**, **d** show a hilly morphology with a height difference of several nanometers. Here, the upper part of (**c**) exhibits a single atomic roughness. **a**, **c** are reprinted with permission from [31]. Copyright © 2022 American Chemical Society

[32]. During the recording of the image, the sample potential (with respect to the RE) was switched such that the HER was allowed ('On') or hindered ('Off'). The latter is achieved at a potential in the double-layer region. For reaction 'On', locally distinct noise features occur, which can be used to assess the geometry of active areas. More details on the working principle of the technique are given in Section '2'. In Fig. 3a, b, near the step sizes, the noise level is higher compared to the Pd(111) terraces. Therefore, we can assume a higher electrochemical activity of these structures. In contrast, the terraces have fewer noise peaks, which indicates lower activity. For the reaction 'Off', which is shown in the middle part of the measurement, the overall noise level of the image

is low. This provides a reference to assign noise to electrochemical activity; and not to a change in morphology. Combining several EC-STM measurements with further mentioned evaluation techniques makes a conclusion on the nature of active sites possible. Here, on Pd(111), we identify the highest accumulation of active sites on the top of the step edges and a lower one on the terrace (cf. reference [28]).

Figure 3c, d provides an analog measurement for Pd(100) in 0.1 M HClO$_4$. During the recording of the image, the sample potential was switched between reaction 'On' and 'Off'. The bottom part of the image shows an elevated structure with rich noise behavior. In contrast, at first glance, the terrace in the upper part exhibits no
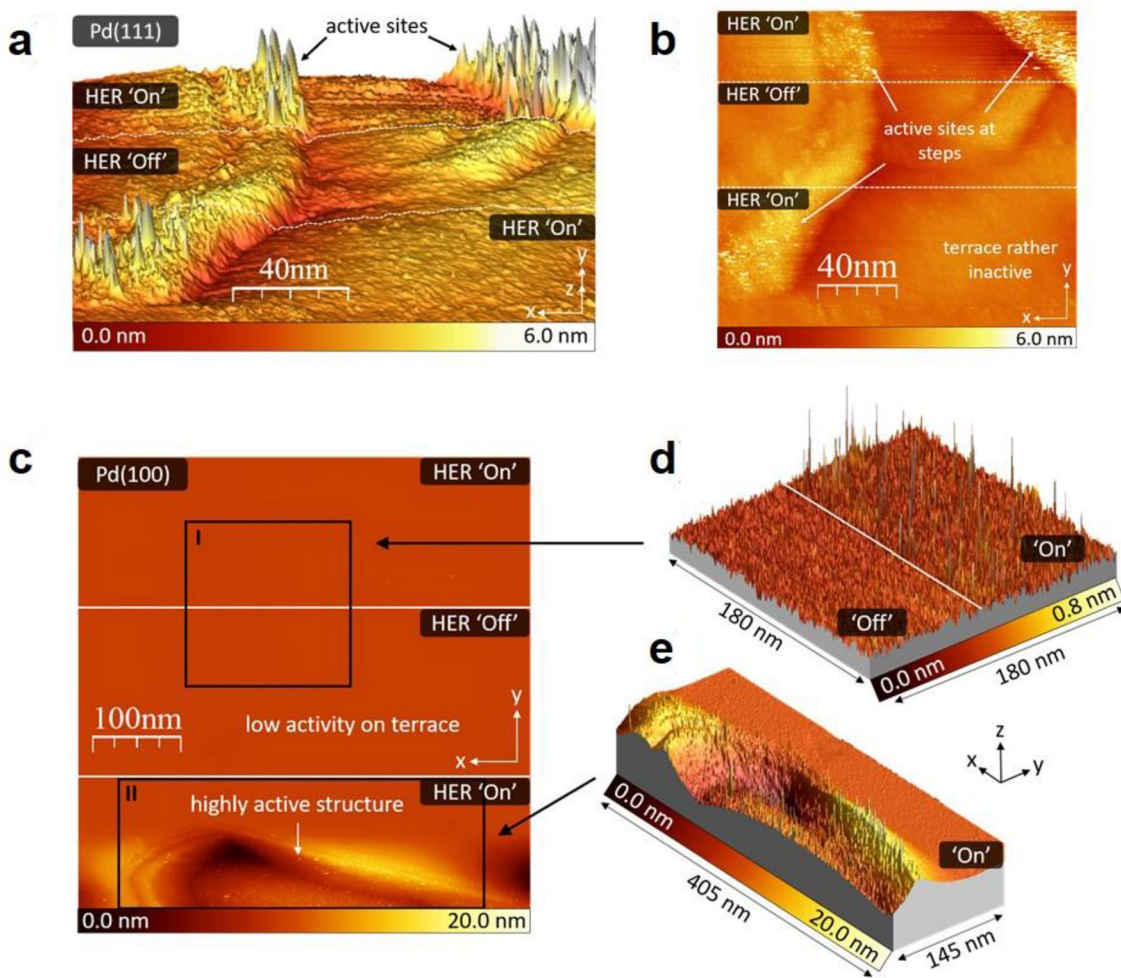
Fig. 3 n-EC-STM measurements on Pd surfaces under HER conditions. **a** Three-dimensional view of an n-EC-STM measurement of freshly annealed Pd(111) in 0.1 M HClO₄. By comparing the signal between reactions 'On' and 'Off', we encounter distinct noise spikes at the active sites. While the flat areas remain mostly inactive, a high noise level. However, at a closer look at the terrace sites accumulation of active sites is visible on the step edges. **b** Two-dimensional view of (**a**). **c** n-EC-STM measurement of annealed Pd(100) in 0.1 M HClO₄. **d** Comparison of reaction 'On' and 'Off' for terrace sites. **e** Active structure, including step sites.

noise level. However, at a closer look at the terrace sites in Fig. 3d, a noise level increase is visible between 'On' and 'Off'. Since the noise level of the terrace is orders of magnitude lower than at the step, the terrace noise is less easily visible in the overall image of Fig. 3c, but can be detected by an individual investigation of this area. Here, it is important to note that a comparison of the noise is only possible within an individual image or a series of line scans, but not between different measurements since several influences like feedback settings, tip properties, or electrolyte concentration can alter the intensity of the noise. From previous measurements (cf. reference [28]), we know that the highest activity on Pd(100) is located on step-edges, while a lower but also significant one is spotted on the terrace as well. This is in good agreement with Fig. 3c–e, as the structure in the lower third of the images

might consist of multiple steps while the activity on the terrace is also elevated.

In summary, for unstrained, as-prepared Pd(111) and Pd(100) surfaces, step sites show higher activity than terrace sites. The explanation is an activity-coordination dependence, which is mentioned at the beginning of the section. For the inclusion of strain effects during hydride formation and for more details on the applied potentials, we refer to reference [28].

4.2 Carbon Surfaces: High-Resolution Imaging Under Reaction Conditions

It has been well-known for a long time that, in principle, the STM is capable of resolving the electronic structure of surfaces with a sub-nanometer resolution. In many cases,
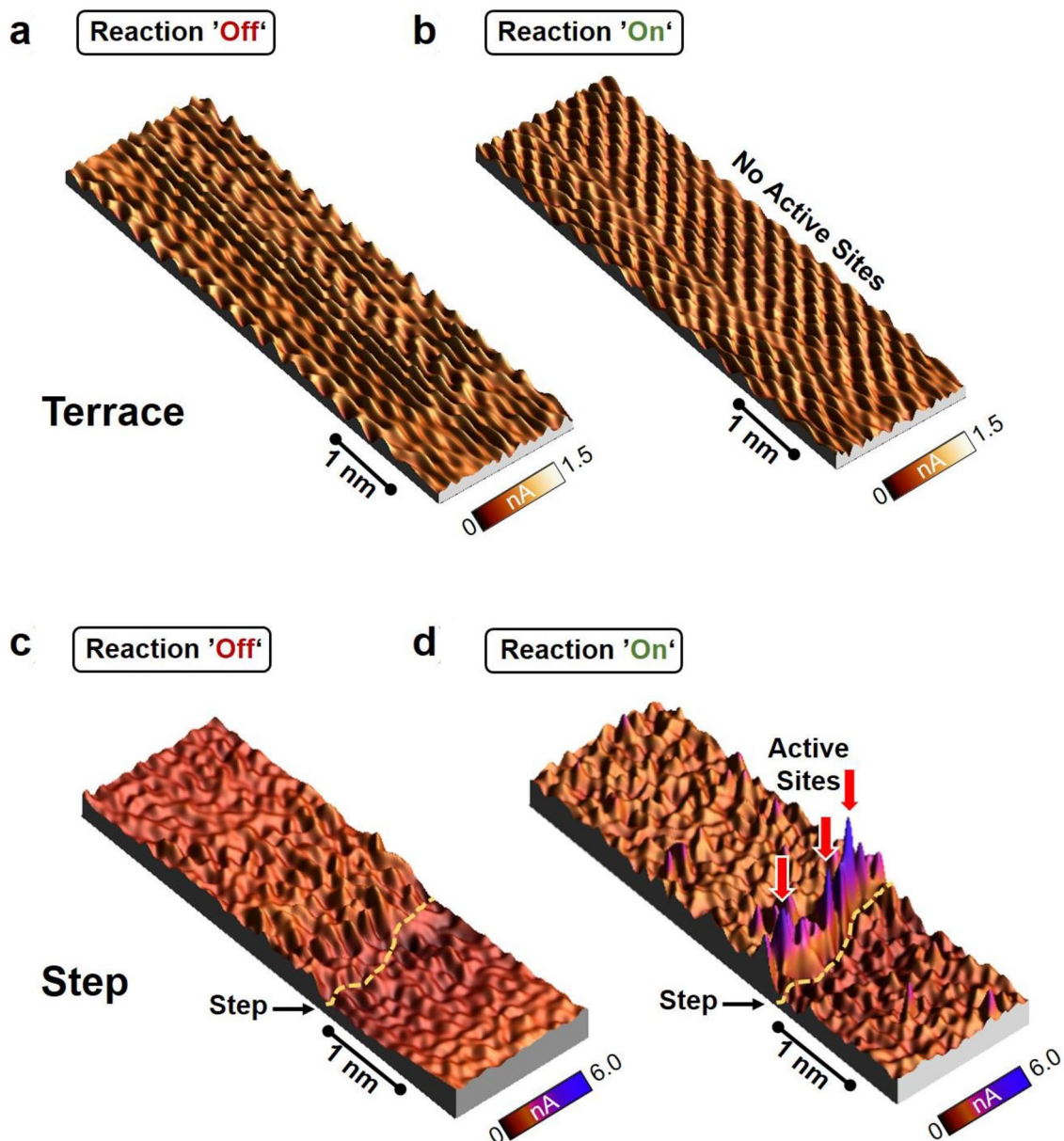
Fig. 4 Atomic-resolution images of HOPG under HER conditions. **a**, **b** Measurement of a HOPG terrace (basal plane) while the applied potential corresponds to **a** reaction 'Off' and **b** reaction 'On' (cf. reference [37] for more information on the applied potentials). No active sites can be detected under the reaction conditions. **c**, **d** represent a repetition of the experiment at a position including a step edge. In this case, the reaction causes noise spikes (in purple color) along the upper edge of the step, indicating the presence of active sites. Reproduced from reference [37] with permission from the Royal Society of Chemistry

the resulting STM image relates to the atomic configuration and is, therefore, often called atomic resolution. One of the first successful applications is the visualization of the Si(111) reconstruction by Binnig and Rohrer, just a few months after their introduction of the STM technique [33]. Naturally, being able to replicate this functionality

under reaction conditions to identify active sites would be a valuable resource. Consequently, we carried out a study specifically targeting achieving the best possible resolution of active sites by using the n-EC-STM method. We selected a simple model system so that the evaluation of the images is straightforward. The sample material was

HOPG, which possesses a highly periodic configuration and is, for this reason, a typical calibration surface for STM measurements. Importantly, it is, for several reasons, also an interesting material for energy conversion devices. First of all, carbon is one of the most abundant materials on earth, and HOPG can be seen as a model system for many carbon-based catalyst structures [34]. Moreover, carbon has good electronic conductivity properties and is often used as a support for nanoparticulate catalysts [35]. Additionally, graphite is employed as an anode material in some batteries, such as Li-ion batteries. In this case, it is desirable to suppress any interfering reactions [36]. Taking these considerations into account, it is clear that knowing the nature of the active sites is the fundament for designing a functional material that, depending on the application, maximizes or minimizes the activity toward a reaction. The reaction we investigated was the HER in an acidic medium (0.1 M HClO$_4$). The advantage of this reaction is a relatively simple mechanism involving only one intermediate (*H). Additionally, it is currently predominantly catalyzed using platinum group metals which are scarce, and it is one of the most common interfering reactions at graphite electrodes in batteries.

To start, we focused on the HOPG basal plane by imaging a section of a large terrace on the sample. The resolution was increased so that the periodic structure of the sample was visible. Then, the same area was captured once with the reaction 'Off' (Fig. 4a) and once with the reaction 'On' (Fig. 4b). In the images, the periodic surface pattern is represented in a 3D view. From this data, it becomes apparent that there are no active sites on the terrace, as there are no noise spikes in the image under reaction conditions. However, certain surface sites need to be active at the applied potential, causing the HER current in the macroscopic cyclic voltammogram (see e.g. reference [35]). Therefore, we investigated another typical structural motif on the HOPG surface, a step edge. The previous experiment was repeated and is displayed in Fig. 4c (reaction 'Off') and Fig. 4d (reaction 'On'), which illustrate excerpts of the measurements published in reference [37]. Here, also 2D views of the entire images are provided. Under reaction conditions, the upper edges showed clear signs of activity in this case, reflected by the noise spikes at these positions (purple color shade in the image). The spikes appear directly or very close to the upper edge of the step, indicating that the first one or two rows of atoms along the edges should contain the most active atomic configurations. The terraces (i.e., the basal plane) remain almost completely inactive. Minor signs of activity could be caused by defects or other structural deviations from the ordered atomic arrangement.

The results were supported by density functional theory calculations, which suggested the most favorable binding conditions for the *H intermediate should be found within the first two rows of atoms along HOPG edges and in the vicinity of carbon vacancies (more details in reference [37]). This is in good agreement with the observations from the n-EC-STM images. Other literature reports on related carbon materials, using both experimental and theoretical approaches, similarly find the most active sites at the edge planes [38–41]. Consequently, it can be assumed that the n-EC-STM technique is indeed capable of the successful identification and visualization of active sites with down to atomic resolution.

5 Conclusion

In the field of electrocatalysis and its applications, such as water electrolysis, the acceleration of the involved reaction kinetics is vital. For structure-sensitive reactions, optimized binding conditions between reaction intermediates and catalyst surface lead to maximal performance. Therefore, for catalyst design strategies, knowledge about the nature of the active sites, which means their electronic and geometric configuration, is important. In doing so, in-situ techniques with high resolution can provide valuable information. One approach is to evaluate noise features in the EC-STM signal to track local activity changes. As an example, we investigated Pd and HOPG surfaces for the HER. For Pd(111) and Pd(100) in 0.1 M HClO$_4$, a significant activity occurs on step edges while a marginal one appears on flat areas. Besides the capabilities of qualitatively identifying the position of active sites and obtaining quantitative information on their relative activities, it is also possible to achieve an atomic resolution with this technique. This was showcased for the HER on HOPG in an acidic medium, where the most active sites were located within the first two rows of atoms along the upper edge of steps. Depending on the experimental conditions, the n-EC-STM technique allows a targeted and comprehensive in-situ investigation of active sites on well-chosen systems down to atomic resolution by selecting the scan size, the examined surface structures, the electrochemical reaction, and the catalyst materials.

Data availability The data supporting the results of this review are available on reasonable request from the last corresponding author A. S. B.

References

1. Peraldo Bicelli L (1986) Hydrogen: a clean energy source. Int J Hydrog Energy 11:555–562. https://doi.org/10.1016/0360-3199(86)90121-7
2. Schlogl R (2010) The role of chemistry in the energy challenge. Chemsuschem 3:209–222. https://doi.org/10.1002/cssc.200900183
3. Zhang L, Chang Q, Chen H, Shao M (2016) Recent advances in palladium-based electrocatalysts for fuel cell reactions and hydrogen evolution reaction. Nano Energy 29:198–219. https://doi.org/10.1016/j.nanoen.2016.02.044
4. Jayaramulu K, Masa J, Tomanec O et al (2017) Nanoporous nitrogen-doped graphene oxide/nickel sulfide composite sheets derived from a metal-organic framework as an efficient electrocatalyst for hydrogen and oxygen evolution. Adv Funct Mater 27:1700451. https://doi.org/10.1002/adfm.201700451
5. Ito Y, Cong W, Fujita T et al (2015) High catalytic activity of nitrogen and sulfur co-doped nanoporous graphene in the hydrogen evolution reaction. Angew Chem 127:2159–2164. https://doi.org/10.1002/ange.201410050
6. Schmidt TJ, Ross PN, Markovic NM (2002) Temperature dependent surface electrochemistry on Pt single crystals in alkaline electrolytes. J Electroanal Chem 524–525:252–260. https://doi.org/10.1016/S0022-0728(02)00683-6
7. Strmcnik D, Lopes PP, Genorio B et al (2016) Design principles for hydrogen evolution reaction catalyst materials. Nano Energy 29:29–36. https://doi.org/10.1016/j.nanoen.2016.04.017
8. Hou S, Kluge RM, Haid RW et al (2021) A review on experimental identification of active sites in model bifunctional electrocatalytic systems for oxygen reduction and evolution reactions. ChemElectroChem 8:3433–3456. https://doi.org/10.1002/celc.202100584
9. Ebejer N, Schnippering M, Colburn AW et al (2010) Localized high resolution electrochemistry and multifunctional imaging: scanning electrochemical cell microscopy. Anal Chem 82:9141–9145. https://doi.org/10.1021/ac102191u
10. Auer A, Andersen M, Wernig E-M et al (2020) Self-activation of copper electrodes during CO electro-oxidation in alkaline electrolyte. Nat Catal 3:797–803. https://doi.org/10.1038/s41929-020-00505-w
11. Garlyyev B, Fichtner J, Piqué O et al (2019) Revealing the nature of active sites in electrocatalysis. Chem Sci 10:8060–8075. https://doi.org/10.1039/c9sc02654a
12. Binnig G, Rohrer H, Gerber C et al (1982) Surface studies by scanning tunneling microscopy. Phys Rev Lett 49:57–61. https://doi.org/10.1103/PhysRevLett.49.57
13. Binnig G, Rohrer H (1983) Scanning tunneling microscopy. Surf Sci 126:236–244. https://doi.org/10.1016/0039-6028(83)90716-1
14. Hugelmann M, Schindler W (2003) Tunnel barrier height oscillations at the solid/liquid interface. Surf Sci 541:L643–L648. https://doi.org/10.1016/S0039-6028(03)00923-3
15. Hugelmann M, Schindler W (2004) In situ distance tunneling spectroscopy at Au(111)/0.02 M HClO4. J Electrochem Soc 151:E97. https://doi.org/10.1149/1.1644141
16. Simeone FC, Kolb DM, Venkatachalam S et al (2008) Tunneling behavior of electrified interfaces. Surf Sci 602:1401–1407. https://doi.org/10.1016/j.susc.2008.01.034
17. Pan J, Jing TW, Lindsay SM (1994) Tunneling barriers in electrochemical scanning tunneling microscopy. J Phys Chem 98:4205–4208. https://doi.org/10.1021/j100067a001
18. Vaught A, Jing TW, Lindsay SM (1995) Non-exponential tunneling in water near an electrode. Chem Phys Lett 236:306–310. https://doi.org/10.1016/0009-2614(95)00223-Q
19. Nagy G, Wandlowski T (2003) Double layer properties of Au(111)/H_2SO_4 (Cl) + Cu^{2+} from distance tunneling spectroscopy. Langmuir 19:10271–10280. https://doi.org/10.1021/la034950k
20. Hiesgen R, Eberhardt D, Meissner D (2005) Direct investigation of the electrochemical double layer using the STM. Surf Sci 597:80–92. https://doi.org/10.1016/j.susc.2004.10.057
21. Calle-Vallejo F, Tymoczko J, Colic V et al (2015) Finding optimal surface sites on heterogeneous catalysts by counting nearest neighbors. Science 350:185–189. https://doi.org/10.1126/science.aab3501
22. Calle-Vallejo F, Pohl MD, Reinisch D et al (2017) Why conclusions from platinum model surfaces do not necessarily lead to enhanced nanoparticle catalysts for the oxygen reduction reaction. Chem Sci 8:2283–2289. https://doi.org/10.1039/C6SC04788B
23. Haid RW, Kluge RM, Liang Y et al (2021) In situ quantification of the local electrocatalytic activity via electrochemical scanning tunneling microscopy. Small Methods 5:e2000710. https://doi.org/10.1002/smtd.202000710
24. Thomas JM (2015) Principles and practice of heterogeneous catalysis, 2, rev. John Wiley & Sons Incorporated, Weinheim
25. Lunardon M, Kosmala T, Durante C et al (2022) Atom-by-atom identification of catalytic active sites in operando conditions by quantitative noise detection. Joule 6:617–635. https://doi.org/10.1016/j.joule.2022.02.010
26. Kosmala T, Baby A, Lunardon M et al (2021) Operando visualization of the hydrogen evolution reaction with atomic-scale precision at different metal–graphene interfaces. Nat Catal 4:850–859. https://doi.org/10.1038/s41929-021-00682-2
27. Nagahara LA, Thundat T, Lindsay SM (1989) Preparation and characterization of STM tips for electrochemical studies. Rev Sci Instrum 60:3128. https://doi.org/10.1063/1.1140590
28. Schmidt TO, Ngoipala A, Arevalo RL et al (2022) Elucidation of structure-activity relations in proton electroreduction at Pd surfaces: theoretical and experimental study. Small 18:e2202410. https://doi.org/10.1002/smll.202202410
29. Haid RW, Kluge RM, Schmidt TO, Bandarenka AS (2021) In-situ detection of active sites for carbon-based bifunctional oxygen reduction and evolution catalysis. Electrochim Acta 382:138285. https://doi.org/10.1016/j.electacta.2021.138285
30. Tymoczko J, Calle-Vallejo F, Schuhmann W, Bandarenka AS (2016) Making the hydrogen evolution reaction in polymer electrolyte membrane electrolysers even faster. Nat Commun 7:10990. https://doi.org/10.1038/ncomms10990

31. Gubanova E, Schmidt TO et al (2022) Structure-dependent electrical double-layer capacitances of the basal plane Pd (hkl) electrodes in HClO4. J Phys Chem C 126:11414–11420. https://doi.org/10.1021/acs.jpcc.2c03117

32. Kibler LA (2003) Preparation and characterization of noble metal single crystal electrode surfaces. Int Soc Electrochem 14:20

33. Binnig G, Rohrer H, Gerber C et al (1983) 7 × 7 reconstruction on Si(111) resolved in real space. Phys Rev Lett 50:120–123. https://doi.org/10.1103/PhysRevLett.50.120

34. Geim AK, Novoselov KS (2009) The rise of graphene. In: Rodgers P (ed) Nanoscience and technology. Co-Published with Macmillan Publishers Ltd, UK, pp 11–19

35. Murthy AP, Madhavan J, Murugan K (2018) Recent advances in hydrogen evolution reaction catalysts on carbon/carbon-based supports in acid media. J Power Sources 398:9–26. https://doi.org/10.1016/j.jpowsour.2018.07.040

36. Strmcnik D, Castelli IE, Connell JG et al (2018) Electrocatalytic transformation of HF impurity to H_2 and LiF in lithium-ion batteries. Nat Catal 1:255–262. https://doi.org/10.1038/s41929-018-0047-z

37. Kluge RM, Haid RW, Stephens IEL et al (2021) Monitoring the active sites for the hydrogen evolution reaction at model carbon surfaces. Phys Chem Chem Phys 23:10051–10058. https://doi.org/10.1039/D1CP00434D

38. Holmberg N, Laasonen K (2015) Ab initio electrochemistry: exploring the hydrogen evolution reaction on carbon nanotubes. J Phys Chem C 119:16166–16178. https://doi.org/10.1021/acs.jpcc.5b04739

39. Xie A, Xuan N, Ba K et al (2017) Pristine graphene electrode in hydrogen evolution reaction. ACS Appl Mater Interfaces 9:4643–4648. https://doi.org/10.1021/acsami.6b14732

40. Das RK, Wang Y, Vasilyeva SV et al (2014) Extraordinary hydrogen evolution and oxidation reaction activity from carbon nanotubes and graphitic carbons. ACS Nano 8:8447–8456. https://doi.org/10.1021/nn5030225

41. Davies TJ, Hyde ME, Compton RG (2005) Nanotrench arrays reveal insight into graphite electrochemistry. Angew Chem Int Ed 44:5121–5126. https://doi.org/10.1002/anie.200462750